Insights from Angle-Resolved Photoemission Spectroscopy of an Undoped Four-Layered Two-Gap High-T_c Superconductor

Wenhui Xie,[1] O. Jepsen,[1] O. K. Andersen,[1] Yulin Chen,[2] and Z.-X. Shen[2]

[1]*Max-Planck Institut für Festkörperforschung, Heisenbergstraße 1, D-70569 Stuttgart, Germany*
[2]*Stanford Synchrotron Radiation Laboratory, Stanford University, Stanford, California 94305, USA*

(Received 7 July 2006; published 22 January 2007)

An undoped cuprate with apical fluorine and inner (i) and outer (o) CuO_2 layers is a 60 K superconductor whose Fermi surface has large n- and p-doped sheets with the superconducting gap on the n sheet twice that on the p sheet. The Fermi surface is *not* reproduced by the local density approximation, but the screening must be substantially reduced due to electronic correlations, *and* oxygen in the o layers must be allowed to dimple outwards. This charges the i layers by $0.01|e|$, causes a 0.4 eV Madelung-potential difference between the i and o layers, quenches the i-o hopping, and localizes the n sheets onto the i layers, thus protecting their d-wave pairs from being broken by scattering on impurities in the BaF layers. The correlation-reduced screening strengthens the coupling to z-axis phonons.

DOI: 10.1103/PhysRevLett.98.047001 PACS numbers: 74.25.Jb, 71.18.+y, 74.72.Jt

Despite 20 years of intensive research, high-temperature superconductivity in the cuprates has not been understood. Much insight has been gained through discoveries of new cuprates and refinements of experimental techniques. An example is the discovery [1,2] of an undoped 4-layered cuprate with apical fluorine, $Ba_2Ca_3Cu_4O_8F_2$ (F0234), which is not a Mott insulator, but a 60 K high-temperature superconductor (HTSC) with two gaps and an anomalous Fermi surface [1].

All HTSCs consist of CuO_2 layers separated by apical blocks into which dopants may be inserted. Undoped cuprates (Cu $3d^9$) are antiferromagnetic (AF) Mott insulators. Upon hole-doping beyond $p \sim 0.05$ per CuO_2, they become HTSCs with pairing symmetry $d_{x^2-y^2}$, and the critical temperature reaches a maximum, $T_{c\,\max}$, when $p \sim 0.2$. For optimally and overdoped materials the Fermi surfaces (FS) measured by angle-resolved photoemission spectroscopy (ARPES) enclose large hole areas of size $1 + p$ (in units of half the Brillouin-zone area), are centered at $(k_x, k_y) = (\pi, \pi)$, and agree surprisingly well with detailed predictions from local density approximation (LDA) band-structure calculations [3]. Even the existence of a small subband splitting in bilayered cuprates [4,5], which is twice the integral for interlayer hopping, $t_\perp(\mathbf{k}_\parallel) \sim t_\perp(\cos k_x - \cos k_y)^2/4$, and the existence of a k_z dispersion proportional to $t_\perp(\mathbf{k}_\parallel)\cos\frac{1}{2}k_x \cos\frac{1}{2}k_y \cos\frac{c}{2}k_z$ in body-centered tetragonal materials [6,7] have recently been confirmed by ARPES [3,8] and angular magnetoresistance oscillations [9]. Hence, overdoped and optimally doped cuprates appear to have well-defined quasiparticle bands with mass renormalizations 2–4 not only in the direction of the layers but also in the perpendicular direction [3,10,11]. For underdoped materials, a pseudogap opens up when $T < T^*$. The remaining Fermi arcs [3,12], when mirrored around the AF zone boundary, enclose *small* hole areas of size p, are centered at $(\frac{\pi}{2}, \frac{\pi}{2})$, and are roughly reproduced by LDA + U calculations with $U_{dd} \sim 6$ eV and AF long-range order, or similar Hartree-Fock solutions for 3-band models [5,13]. Upon doping with electrons beyond a certain level, a metallic AF (AFM) phase develops and, subsequently, a superconducting phase with the electrons occupying small, $(\pi, 0)$-centered FS areas of size n. For higher n doping [3,14], antiferromagnetism disappears and the FS again becomes (π, π) centered and large, of size $1 - n$. Optimal n doping occurs for $n \sim 0.2$, and known values of $T_{c\,\max}$ are much smaller ($\lesssim$40 K) than for optimal p doping ($\lesssim$140 K), and so are the gaps.

In Fig. 1, we show the FS of undoped F0234. ARPES resolves the two sheets shown in gray [1]. Both are (π, π) centered and large, their areas being $1 \pm p$ with $p \sim 0.2$. We shall refer to the larger one as the hole-doped or p sheet and to the smaller one as the electron-doped or n sheet. F0234 thus appears to be the first *self-doped* HTSC having n and p doping in one and the same crystal. All other known undoped cuprates, single layered as well as multilayered, are insulating, and when hole doped, the observed FS-area splittings [8] are almost an order of magnitude smaller than the ± 0.2 found in F0234. We shall try to answer the following questions in this Letter: How and why does this compound manage to dope itself?

There are no FS measurements for multilayered cuprates with inequivalent inner (i) and outer (o) layers, with the exception of F0234, but *site-selective* NMR studies [15] indicate that i layers have less holes than o layers and that superconductivity develops differently with temperature in the different layers. This behavior is interpreted in terms of electrons localized onto individual layers, each of which follows the generic phase diagram as a function of doping, and which are weakly coupled by proximity effects [16]. Most spectacular are the properties of 5-layered $HgBa_2Ca_4Cu_5O_{12+\delta}$ [17]. Here, the o layers form an optimally doped HTSC with $T_{c\,\max} = 108$ K and the three i layers are AF *metals* (AFM) with moments of about $0.3\mu_B$.

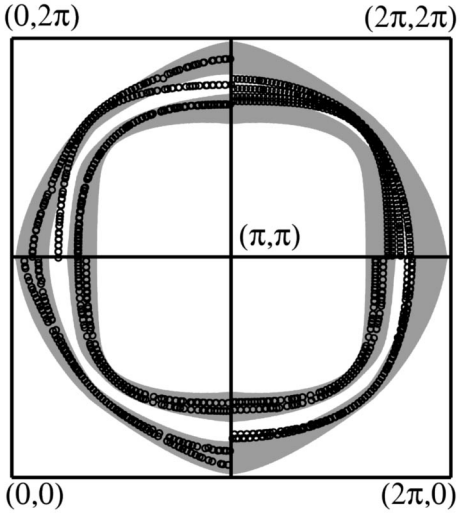

FIG. 1. FS for F0234. Gray: ARPES [1]. The width reflects the experimental error bar. The smaller (larger) sheet is the n (p) sheet. Open dots: Calculations. Top right: LDA. Remaining three quarters: $\langle \mathrm{LDA} + U \rangle$. Bottom right: Flat CuO_2 layers and 2% F-O exchange ($q = 0.02$) treated in the VCA. Indistinguishable from this FS are the ones calculated with no F-O exchange, but with oxygen in the o or i layers dimpled outwards by 0.07 Å. See Fig. 2. The n (p) sheet resides on the i (o) layers. ε_F is adjusted such the FS fits along the nodal line, whereby $n = 0.19$ and $p = 0.12$. Bottom left: Dimpling as before, but with the vertical Ba and F positions adjusted such as to give the best agreement with the ARPES FS: $z_{\mathrm{Ba}} - z_{\mathrm{Cu}_o}$ is decreased from 2.0 to 1.7 Å and $z_F - z_{\mathrm{Cu}_o}$ is decreased from 2.4 to 2.1 Å. ε_F is adjusted as before, whereby $n = 0.18$ and $p = 0.21$. Top left: As before, but with O in the o (or i) layers dimpled inwards by 0.10 Å. Now, the n (p) sheet resides on the o (i) layers. $z_{\mathrm{Ba}} - z_{\mathrm{Cu}_o} = 1.6$ Å and $z_F - z_{\mathrm{Cu}_o} = 2.0$ Å. ε_F is adjusted as before, whereby $n = 0.15$ and $p = 0.18$. Note that intersheet splittings in $\mathbf{k}$ space are enhanced near the saddle points in the band structure.

By decreasing the hole doping, T_c decreases to 70 K and the o layers form a uniformly mixed HTSC-AFM phase with $0.1\mu_B$ moments, while the i layers form a $0.7\mu_B$ AFM. The layers are flat and the estimated hole counts for the o and i layers differ by as much as 0.2 for the overdoped material.

Seen on the background of these truly exotic properties, the discovery [1] that F0234 is the first HTSC with different SC gaps on the two sheets may seem less spectacular. However, it is the gap on the n sheet which is the largest, actually twice the gap on the p sheet, and this is opposite to what one would expect from the generic phase diagram. Moreover, two-gap superconductivity has only been observed unambiguously in a few materials of which MgB_2 is the most spectacular. There, the mechanism is conventional [18,19].

Whereas the FS sheets observed in all other multilayered HTSCs are hardly split along the nodal direction, F0234 exhibits a large nodal splitting, $\Delta k_{[110]}$. This is the third anomaly of the ARPES data and the key to the self-doping and the two gaps. For comparison with the ARPES FS, we show in the top right-hand quarter of Fig. 1 the LDA FS which is seen to have four FS sheets, split almost exclusively by interlayer hopping [20]. The four subbands are split by approximately $\pm\frac{1}{2}(\sqrt{5} \pm 1)t_\perp(\mathbf{k}_\parallel)$ with $t_\perp \sim 0.2$ eV. This is the first case known to us where there is a substantial discrepancy between an experimental, large FS and the LDA. The latter fails to reproduce the $\Delta k_{[110]}\partial\varepsilon/\partial k_{[110]} = 0.4$ eV large Madelung-potential difference (on electron scale) between the layers on which, respectively, the p- and the n-nodal quasiparticles are located. We have taken $\partial\varepsilon/\partial k_{[110]}$ as the bare (LDA) nodal velocity, which is the consistent choice in the present context [21]. In the LDA [and generalized gradient approximation (GGA)], the electron potential averaged over an i layer is merely 0.024 eV (0.034 eV) below that averaged over an o layer—that is 17 (12) times too little. The discrepancy remains after we optimize the structure using the LDA. Thereby, most notably, the oxygens in the o layers dimple outwards by $\sim 3°$, about one-third the dimple in $YBa_2Cu_3O_7$ [22].

Since the 0.4 eV potential exceeds $\frac{1}{2}(\sqrt{5} + 1)t_\perp$, it effectively blocks the hopping between the i and the o layers. Therefore, the n sheets are associated with the i layers and the p sheets with the o layers, or the other way around. The potential difference thus blocks interband scattering and protects the i bands from scattering on the ubiquitous impurities in the apical BaF blocks. This may be the reason why two SC gaps survive and—in case the p sheets reside on the o layers—also the reason why the gap on the p sheets is the smaller one: it is suppressed by scattering on impurities in the BaF block.

Let us set this 0.4 eV potential difference in perspective: With the in-plane lattice constant 3.86 Å and the distance between Ca and CuO_2 layers 1.54 Å, Poisson's equation says that the layer-averaged potential is a sawtooth with kinks of ~ 20 eV Q_n on the layers. Q_n is the charge per 2D cell. If F0234 were purely ionic, the potential would therefore be 0 on the Ca^{2+} layers and 20 eV on the $(CuO_2)^{2-}$ layers, the same on the i and o layers because the $CaCuO_2$ unit is neutral. Next, we transfer from the BaF layers q_i positive charges to each of the i layers and q_o positive charges to each of the o layers. This sets up a difference in Madelung potential between o and i layers of $40q_i$ eV, which depends only on q_i, not on q_o because the i layers are next to the Ca mirror plane [23]. The ARPES value of 0.4 eV (neglecting exchange-correlation contributions) therefore tells us that the i layers have a net charge of either $0.01|e|$, in which case the n sheets reside on the i layers, or of $-0.01|e|$, in which case the p sheets are on the i layers. In the LDA (GGA), the charging is 17 (12) times smaller.

Crystallographically it is possible that q of the two layer oxygens per cell are exchanged with fluorine, so that the formula is $Ba_2Ca_3(CuO_{2-q}F_q)_4O_{4q}F_{2-4q}$. In fact, LDA calculations with $q = 0.25$, employing not only the virtual-crystal approximation (VCA) but also supercells,

do reproduce the ARPES FS. However, since the position of the F $2p$ level is below that of O, such impurities in the CuO_2 layers are very efficient in breaking $d_{x^2-y^2}$-wave pairs: For an allowed T_c suppression of 10%, we find that q cannot exceed 0.001, which is even smaller than the charging of 0.01 needed to create the observed crystal-field splitting in the absence of screening [24]. This rules out F-O exchange as an explanation for the anomalous ARPES FS.

Quantum Monte Carlo calculations for a t_{1u}-band Hubbard model for C_{60} have revealed that the RPA describes metallic screening well for $U/W \lesssim 2$, but that once $U/W \sim 3$, electronic correlations reduce the screening by an order of magnitude [25]. This seems to be the problem with the LDA when applied to F0234, which is even nearly two dimensional. One might think of reducing all interlayer hoppings as was recently done using the Gutzwiller approximation [26], but this would not directly change the metallic interlayer screening, $1 + 2NM \sim 25$, where $2N \sim 0.6$ electrons/(eV · CuO_2) is the intralayer density of states at the Fermi level and $M \sim 40$ eV · CuO_2/electron is the interlayer Madelung constant. Instead, we perform self-consistent LDA + U calculations for AF (π, π) order and subsequently calculate the band-structure and FS for the charge potential, neglecting the spin potential. We denote this procedure as $\langle \mathrm{LDA} + U \rangle$. The result for the pure compound ($q = 0$) is very similar to that obtained by the LDA and shown in the top right-hand quarter of Fig. 1. However, with an F-O exchange corresponding to $q = 0.02$, we do obtain the proper splitting along the nodal line. This is shown in the bottom right-hand quarter of Fig. 1. The $\langle \mathrm{LDA} + U \rangle$ procedure thus reduces the screening of this perturbation to about $0.02/0.01 = 2$, but the pair-breaking argument of why F-O exchange is an unlikely explanation for the anomalous ARPES FS remains valid. So from now on, we take $q = 0$.

Next, we include the calculated outwards dimple of the outer O_2 layer (see Fig. 3), which is about the same in the LDA and the LDA + U. That this may induce a potential shift between the i and o layers can be seen as follows: For the calculated $0.07–\frac{1.54}{20}$ Å dimple, the bare value of the Madelung potential between the split Cu^{2+} and $(O^{2-})_2$ sublayers of the o layer is $\frac{3\times 20\ \mathrm{eV}}{20} = 3$ eV, and after averaging over the sublayers this yields a 2 eV bare Madelung shift of the o layer with respect to the i layer. Figure 2 shows the $\langle \mathrm{LDA} + U \rangle$ layer-averaged potential for all the Raman-active (even) dimples of the i and o layers. We see that the intralayer screening is substantial, that the interlayer screening is about $\frac{2\ \mathrm{eV}}{0.5\ \mathrm{eV}} = 4$, and that for the calculated equilibrium structure the $\langle \mathrm{LDA} + U \rangle$ creates the proper 0.4 eV potential. The FS is very similar to the one in the bottom right quarter of Fig. 1. Essentially the same FS is obtained by dimpling the i layers outwards. In all cases, the n sheets are on the i layers and split by the hopping between them. The p sheets are on the o layers and almost degenerate; they agree less well with ARPES

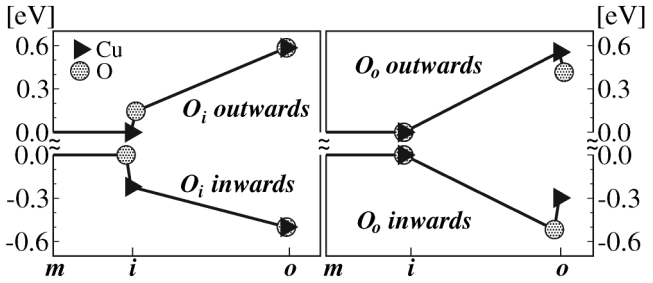

FIG. 2. Layer-averaged potentials calculated with $\langle \mathrm{LDA} + U \rangle$ for dimplings of ±0.1 Å of the inner (left) and outer (right) layer oxygens. This potential is the calculated Cu and O core levels, lined up on the layer which is not dimpled, and normalized to zero at the Ca mirror plane (m).

near the antinodal direction where the ARPES peaks are less well defined. Moreover, the ARPES data have been forced to yield the area, $1 \pm p$, proper for zero doping, which for the real material may not hold exactly. We have chosen to shift the Fermi level to fit ARPES along the nodal direction. In the bottom left-hand quarter of Fig. 1 we demonstrate that perfect agreement with ARPES can be obtained by adjustment of the vertical Ba and F positions.

If—in disagreement with the total-energy result—we dimple the o layers or the i layers inwards by 0.1 Å, the FS shown in the top left-hand quarter of Fig. 1 is obtained. Now the n sheets are on the o layers and unsplit, whereas the p sheets are on the i layers and split by the hopping between them.

There has recently been interest in possible consequences of poor z-axis screening for the electron-phonon interaction at small momentum transfers [27,28]. We note that the coupling of the FS to an a_{1g} Raman-active dimpling mode via the screened Madelung-potential difference (once it exceeds the interlayer hopping) is proportional to the Cu-O_2 distance, rather than to this distance squared, as is the case for the hopping-induced coupling considered earlier [29]. From Fig. 2 we realize that the deformation potential is sizeable: $D = 5$ eV/Å. For a rough estimate of the associated electron-phonon coupling, let us as in Ref. [19] use the Hopfield expression, $\lambda = ND^2/(M\omega^2)$, to compare with MgB_2 for which $\lambda \approx 1.0$: In F0234, the density of states appropriate for $d_{x^2-y^2}$ pairing is twice the value in MgB_2, D is 2.5 times smaller, and $M\omega^2$ is 1.3

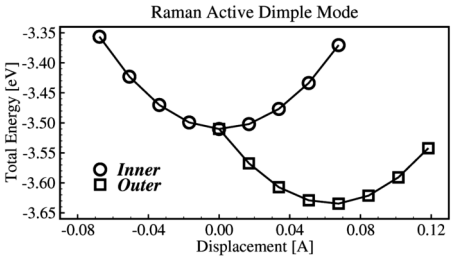

FIG. 3. Total energy as a function of the Raman-active dimpling displacements calculated with LDA + U. See Fig. 2.

times smaller for a Raman-active oxygen dimpling mode than for the optical bond-streching mode in MgB_2. Finally, the strong screening for large momentum transfers in F0234 effectively limits the integrand to the central half of the 2D Brillouin zone. As a result, $\lambda \sim \frac{1}{3}$, which suffices to enhance some other mechanism for HTSC.

We have shown how undoped F0234 manages to self-dope: by a dimpling distortion which is screened out poorly due to strong electronic correlations. This sets up a 0.4 eV difference in Madelung potential between the outer and inner layers, and that causes the FS to split along the nodal direction. The large Madelung-potential difference prevents interband scattering, and that seems to be the reason why two SC gaps survive. Since the dimpling is outwards according to our total-energy linear augmented-plane-wave (LAPW) calculations, both in the LDA and in the LDA + U, the FS sheet with the small gap, the p sheet, is located on the outer layers, next to the BaF blocks where impurities are ubiquitous. This suggests that the p gap is small because it is suppressed by impurity scattering, while the n sheet is protected by the Madelung potential. The phase-diagram model, on the other hand, predicts the p gap to be the largest. A further reason for the different gap sizes could be that, like in MgB_2 [18,19], (one of) the interaction(s) driving the superconductivity is stronger for the n than for the p sheet. It could be of relevance that the bonding n sheet has a larger effective intralayer second-nearest neighbor Cu-Cu hopping integral, $t' + \frac{1}{8}t_\perp \sim 0.39t$, than the p sheet, for which the effective value is merely $t' \sim 0.33t$, and therefore nests better along the [10] directions. This would be consistent with the observation that for hole-doped multilayer cuprates $T_{c\,\max}$ correlates positively with the largest sheet value of t'/t [6].

Why these anomalies have been observed only in F0234 is undoubtedly due to the apical ions being F rather than O. Presumably, when going from apical O to the more ionic F, the covalency between Ba and the apical ion is reduced, whereby the covalency between Ba and O in the o layer is strengthened and causes it to dimple towards Ba.

It will be interesting to follow the development of the $Ba_2Ca_3Cu_4O_8(F_{1-2p}O_{2p})_2$ FS and its SC gaps as a function of hole-doping p. If our assignment of the p sheets with the o layers is correct, and as long as screening remains poor, O doping should suppress the gap on the p sheet. Currently it is known that $T_{c\,\max} = 105$ K is reached at $p = 0.20$ [2], but no ARPES data are available.

We are grateful to O. Gunnarsson and J. Zaanen for useful discussions.

[1] Y. Chen *et al.*, Phys. Rev. Lett. **97**, 236401 (2006).
[2] A. Iyo *et al.*, Physica (Amsterdam) **392C–396C**, 140 (2003); Supercond. Sci. Technol. **17**, 143 (2004).
[3] A. Damascelli *et al.*, Rev. Mod. Phys. **75**, 473 (2003).
[4] S. Chakravarty *et al.*, Science **261**, 337 (1993).
[5] O. K. Andersen *et al.*, J. Phys. Chem. Solids **56**, 1573 (1995).
[6] E. Pavarini *et al.*, Phys. Rev. Lett. **87**, 047003 (2001).
[7] S. Sahrakorpi *et al.*, Phys. Rev. Lett. **95**, 157601 (2005).
[8] D. L. Feng *et al.*, Phys. Rev. Lett. **86**, 5550 (2001); Y.-D. Chuang *et al.*, Phys. Rev. Lett. **87**, 117002 (2001); A. A. Kordyuk *et al.*, Phys. Rev. B **66**, 014502 (2002).
[9] N. E. Hussey *et al.*, Nature (London) **425**, 814 (2003).
[10] T. K. Kim *et al.*, Phys. Rev. Lett. **91**, 167002 (2003); A. Koitzsch *et al.*, Phys. Rev. B **69**, 140507(R) (2004).
[11] *Observed* mass renormalizations are small and isotropic compared with those predicted by a one-band-per-layer Hubbard model with $U = 3.2$ eV and LDA parameters, solved in the fluctuation-exchange approximation; A. I. Liechtenstein *et al.*, Phys. Rev. B **54**, 12 505 (1996).
[12] A. G. Loeser *et al.*, Science **273**, 325 (1996).
[13] R. S. Markiewicz and A. Bansil, Phys. Rev. Lett. **96**, 107005 (2006).
[14] N. P. Armitage *et al.*, Phys. Rev. Lett. **88**, 257001 (2002).
[15] Y. Tokunaga *et al.*, Phys. Rev. B **61**, 9707 (2000); H. Kotegawa *et al.*, J. Phys. Chem. Solids **62**, 171 (2001).
[16] S. Chakravarty *et al.*, Nature (London) **428**, 53 (2004); M. Mori and S. Maekawa, Phys. Rev. Lett. **94**, 137003 (2005).
[17] H. Kotegawa *et al.*, Phys. Rev. B **69**, 014501 (2004); H. Mukuda *et al.*, Phys. Rev. Lett. **96**, 087001 (2006).
[18] I. I. Mazin *et al.*, Phys. Rev. Lett. **89**, 107002 (2002).
[19] L. Boeri *et al.*, Phys. Rev. Lett. **93**, 237002 (2004).
[20] We used the WIEN2K implementation [K. Schwarz *et al.*, Comput. Phys. Commun. **147**, 71 (2002)] of the LAPW method with the Ceperley-Alder LDA xc potential as well as with the LDA + U scheme. $s_{\mathrm{Ca,Ba,Cu,O,F}} = 2.5$, 2.6, 1.9, 1.7, 1.8 Bohr radii, $K_{\max} s_{\mathrm{O}} = 7.5$, $l_{\max} = 10$, and $U_{dd} = 5.4$ eV.
[21] Going $\Delta k_{[110]}$ away from a FS sheet, the corresponding ARPES band first slopes ~3 times less and then, after a kink at ~0.07 eV, about the same as the LDA band.
[22] M. A. Beno *et al.*, Appl. Phys. Lett. **51**, 57 (1987).
[23] Similarly, the difference in the Madelung potential between the BaF and the o layer depends only on the charge $-(q_o + q_i)$ on the BaF layer.
[24] Like in G. Haran and A. D. S. Nagi, Phys. Rev. **54**, 15 463 (1996), we find for small concentrations, q, of fluorine substituting for layer oxygen $T_c \ln(T_c/T_{c0}) \approx -(\pi/2)^2 \delta^2 q N[\bar{c}^2\overline{c^2e^2} - (\overline{c^2e})^2]$, where $\delta \approx 5$ eV is the level shift, $N \approx 0.5$ states/eV/spin/CuO_2, $c^2(\mathbf{k})$ is the oxygen character of a Bloch state, $e(\mathbf{k})$ is the gap anisotropy normalized such that $\bar{e}^2 \equiv 1$, and an overbar denotes the average over a FS sheet. For the latter and for $c^2(\mathbf{k})$ we used the 4-orbital model [5] [O. K. Andersen (unpublished)].
[25] E. Koch *et al.*, Phys. Rev. Lett. **83**, 620 (1999).
[26] M. Mori *et al.*, J. Phys. Soc. Jpn. **75**, 034708 (2006).
[27] O. Rösch *et al.*, Phys. Rev. Lett. **95**, 227002 (2005).
[28] W. Meevasana *et al.*, Phys. Rev. Lett. **96**, 157003 (2006).
[29] D. J. Scalapino, Phys. Rep. **250**, 329 (1995); S. Y. Savrasov and O. K. Andersen, Phys. Rev. Lett. **77**, 4430 (1996); O. K. Andersen *et al.*, J. Low Temp. Phys. **105**, 285 (1996); O. Jepsen *et al.*, J. Phys. Chem. Solids **59**, 1718 (1998).